Microscopic origin of the magneto-optical properties of CoPt alloys

L. Uba,* S. Uba, and V. N. Antonov†
Institute of Experimental Physics, University of Bialystok, Lipowa 41, PL-15-424 Bialystok, Poland

A. N. Yaresko†
Max-Planck Institute for the Chemical Physics of Solids, D-01187 Dresden, Germany

R. Gontarz
Institute of Molecular Physics, Polish Academy of Sciences, Smoluchowskiego 17, PL-60-179 Poznan, Poland
(Received 20 March 2001; published 6 September 2001)

The microscopic origin of the magneto-optical (MO) properties of Co_xPt_{1-x} alloys is studied on the basis of Kerr effect measurements and first-principles band-structure calculations in a wide range of photon energy ($\hbar\omega = 0.75-5.8$ eV) and Co content ($x = 0.03-0.5$). Spin-polarized relativistic linear-muffin-tin-orbital (LMTO) calculations performed within the local density approximation and supercell approach reproduce well the spectral shape of the measured off-diagonal optical conductivity tensor components. Using the *ab initio* LMTO band-structure calculations, the band-by-band and **k**-space decompositions as well as the analysis of the magneto-optical transitions between electronic states localized in different energy regions are performed. It is found that for the alloys studied the uv part of the MO spectra with a pronounced peak at 4 eV photon energy comes from optical transitions between initial and final states located within well-defined energy intervals that are very close to those obtained for fcc Pt metal in external magnetic field. The correlation between the band structure of the alloys and the energy dependence of their MO spectra is investigated. The importance of the spin-orbit interaction for the transitions in different energy regions is demonstrated by calculating the state- and site-projected density of the expectation value of the orbital moment. The evolution of the electronic structure of Co-Pt alloys with the increase of Co content and the influence of the hybridization between the Co and Pt electronic states are analyzed and discussed.

DOI: 10.1103/PhysRevB.64.125105 PACS number(s): 78.20.Ls, 71.20.Be

I. INTRODUCTION

Since its commercial appearance in 1989, magneto-optical recording has established its status as a removable and erasable disk system with a high recording density. Among many different systems the Co-Pt compounds receive significant attention as a high-density MO recording medium, owing to their large perpendicular magnetic anisotropy, high remanence, capability of stable, and smoothly bordered magnetic domain formation, and high readout efficiency, given by the material parameters R (reflectivity) and θ_K (Kerr rotation). The Co-Pt alloy phase diagram reveals a continuous series of solid solution with the ferromagnetic order over nearly the whole range of concentrations[1] with three well-established ordered phases: CoPt known as the tetragonal $L1_0$ structure and $CoPt_3$ (Co_3Pt) with the cubic $L1_2$ structure. Many experimental and theoretical studies have been done especially for the ordered alloys [2–14] and it is established that the large magneto-optical Kerr effect (MOKE) of the Co-Pt systems is caused by an interplay between the exchange splitting of Co and the spin-orbit (SO) coupling of Pt in the hybridized bands.[6] To understand deeper how the spin-orbit coupling and the exchange splitting work in the systems when the alloy composition changes in a wide range, a detailed analysis of the band structure evolution is desirable.

The characteristic feature of the experimental Kerr rotation spectra of Co-Pt compounds is a pronounced peak in the uv range at around 4 eV. Such a peak is observed also in Fe-Pt alloys and in multilayered structures of Pt with Co, Fe, and Ni (see, e.g., Refs. 15–20, and references therein). As has been recently shown,[21] pure paramagnetic Pt metal in an external magnetic field also exhibits the same feature in the uv spectral range, and the peak in the Kerr rotation spectrum of paramagnetic Pt is closely related to that observed at the same energy in ferromagnetic strongly diluted $Co_{0.07}Pt_{0.93}$ alloy. In both cases the MO response is mainly due to the spin polarization of Pt atoms, notwithstanding that the sources of the spin polarization (and underlying microscopic mechanisms) are different in both cases. However, the physical nature of this behavior has not been studied in detail. In principle, a close relationship between peaks in pure Pt and strongly diluted Co-Pt alloys can be expected, but it is not so obvious for alloys with Co concentration up to 50%. The present study is aimed at an experimental and theoretical investigation of the compositional dependence of the MOKE enhancement in the uv range characteristic for Co-Pt alloys. Also, we attempt to explain to what extent the MO spectra of the alloys are governed by the MO activity of Pt. Particular attention is paid to a microscopic analysis of the mechanisms responsible for the change of the MO spectra as a function of alloy composition.

The electronic structure, optical, and MO spectra for the model alloys of different compositions were investigated on the basis of *ab initio* band-structure calculations. Good agreement between the theory and the experiment has been found. To explain the relations between the shape of the Kerr spectra and the electronic band structure, theoretically calcu-

lated spectra are analyzed using decomposition into contributions corresponding to the transitions between different initial and final states. A band-by-band decomposition of the interband transitions localized around different symmetry points in the Brillouin zone (BZ) is also applied. This allows us to identify the main electronic transitions responsible for the uv peak in Co-Pt alloys.

The paper is organized as follows. The description of the experimental procedure and the theoretical framework is provided in Sec. II. Section III presents the experimental and theoretical MO spectra of Co-Pt alloys. The theoretical analysis of the electronic structure and MO properties of Co-Pt alloys in correlation with those of paramagnetic Pt in an external magnetic field is presented in Sec. IV. Finally, the results are summarized in Sec. V.

II. EXPERIMENTAL AND THEORETICAL DETAILS

The Co-Pt alloy films under study have been prepared by face-to-face dc sputtering on glass substrates in an automated and computer-controlled deposition system. Typical sputtering conditions and other technical details can be found in Ref. 22. The film structure was determined by standard Θ-2Θ x-ray diffraction (XRD). As was inferred from XRD measurements the films studied exhibit weak fcc (111) texture. The alloy compositions were determined by x-ray fluorescence analysis with an energy dispersive x-ray (EDX) system.

The polar Kerr rotation (θ_K) and ellipticity (η_K) spectra were measured at temperature 290 K with a magneto-optical spectrometer based on the polarization modulation technique[23] in the photon energy range 0.75–5.8 eV. The angle of incidence of the light on the sample surface mounted inside of the 1.8-T water-cooled electromagnet was 3°. Details of the MO spectrometer used can be found in Refs. 5,21, and 24. The setup is fully automated and computer controlled via a data acquisition system and was also used to measure θ_K and η_K hysteresis loops at fixed light wavelength. The sensitivity of the Kerr spectrometer is of the order of 10^{-4}–10^{-5} deg (depending on the photon energy and corresponding photon shot noise). The optical properties—refractive index n and extinction coefficient k—have been measured by spectroscopic ellipsometry using the rotating analyzer method[25] in the spectral range 0.75–5.8 eV. The angle of incidence has been set at 67°, optimized as the averaged principal angle of incidence for the measured samples and the spectral range used. The average error in the determination of n and k values is of the order of 0.003.

Self-consistent band-structure calculations were carried out using the spin-polarized relativistic (SPR) linear-muffin-tin-orbital (LMTO) method.[26] The detailed description of the relativistic extension of the LMTO method has been given elsewhere.[27] The four-component basis functions were constructed starting from the solution of the single-site Dirac equation for the spin-independent part of the effective one-electron potential. The matrix elements of the effective magnetic field were incorporated into the Hamiltonian at the variational step as proposed in Ref. 28. This choice of the basis functions makes it straightforward to construct the (third-order) LMTO Hamiltonian and to include the combined corrections to the atomic sphere approximation (ASA),[26] which are necessary to calculate accurately the conductivity tensor in a wide energy interval (Ref. 29; see also Ref. 30). A basis consisting of *s, p, d,* and *f* LMTO's was used. Core-charge densities were recalculated at every iteration of the self-consistency loop. The **k**-space integrations were performed with the improved tetrahedron method[31] and charge self-consistency was achieved within the range of 1000–2000 irreducible **k** points.

III. EXPERIMENTAL RESULTS AND COMPARISON WITH THEORY

To discuss the microscopic origin of the compositional dependence of the MO response in Co-Pt compounds and its correlation with that observed in pure Pt metal we have measured optical and MO spectra for the series of Co_xPt_{1-x} alloy films with Co content increasing from 3.5% up to 48%. The measurements of the field dependence of the MOKE have shown that all the alloys are ferromagnetic at the measured temperature of 290 K except for those with small Co concentration ($x \leqslant 0.06$) which are found to be paramagnetic. In Fig. 1(a) the MO spectra of Pt metal[21] and Co_xPt_{1-x} alloys with $x \leqslant 0.06$ measured in the external magnetic field of 1.5 T at 290 K are presented. As can be seen, the θ_k magnitude is very small and increases from 1.5 mdeg in Pt up to 8 mdeg in $Co_{0.06}Pt_{0.94}$ alloy. The increase of the θ_k magnitude with Co content is explained by the fact that the field-induced MOKE is related to the paramagnetic susceptibility and depends linearly on the induced magnetization.

In Figs. 1(b) and 1(c) the evolution of the θ_k spectra of those Co_xPt_{1-x} alloys that exhibit magnetic ordering at the measured temperature 290 K is presented. The spectra display two well-known features.[32] There is a prominent broad negative peak in the uv region and a smaller one in the ir range. The characteristic peak around 4 eV in the θ_k spectrum is present for all Co_xPt_{1-x} alloys studied and its amplitude increases from 0.017 up to 0.61 deg when the Co amount changes from $x=0.07$ to $x=0.48$. At the same time, the amplitude of fcc Co θ_k spectra in the uv energy range included for comparison in Fig. 1(c) approaches the value of 0.43 deg and changes its sign at 5.1 eV. As one proceeds from Pt to $Co_{0.48}Pt_{0.52}$ alloy, a relatively strong change of the θ_k spectra in the ir spectral range is observed and an appearing peak correlates with the peak at 1.5 eV in Co. The observed strong decrease in the θ_k magnitude of the alloys with the decrease of Co content is due to a drop in magnetization and reflects the Curie temperature reduction. It is interesting to note that both ferromagnetic Co and paramagnetic Pt metals exhibit the θ_k peak at 3.8 eV. However, from the observed compositional dependence of the θ_k spectra the conclusion can be drawn that the pronounced θ_k peak at 4 eV in Co-Pt alloys is mostly correlated with the corresponding peak in pure Pt metal. The detailed analysis of the band structure and identification of the states underlying the optical transitions responsible for the peak can help us to verify this conclusion.

To describe the compositional dependence of the MO

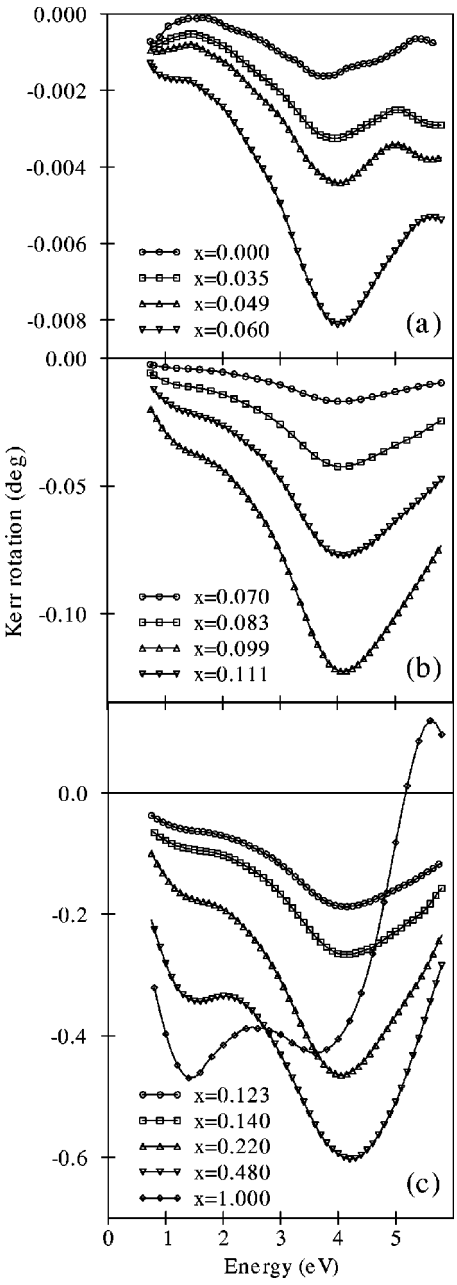

FIG. 1. The polar Kerr rotation measured for Co_xPt_{1-x} alloys of different compositions (indicated in the legends).

properties of the alloys studied, the supercell calculation approach was used. The band structure and MO spectra were calculated for a number of model-ordered structures ($CoPt_{31}$, $CoPt_{15}$, $CoPt_7$, Co_2Pt_{10}, $CoPt_3$, Co_3Pt_5, and CoPt) of different composition. The sequence corresponds to a variation of the Co content in the range of 3–50 %. The crystal structure types, corresponding space groups, and lattice constants of the alloys are presented in Table I. The experimental lattice constants were used in the calculations for all the alloys (for the disordered $Co_{0.25}Pt_{0.75}$ and $Co_{0.48}Pt_{0.52}$ alloys the lattice constants agree with those published in Refs. 35 and 36, respectively). For $CoPt_7$ and $CoPt_3$ alloys, cubic and tetragonal lattices with unit cells with different c/a ratios were studied. For other alloys cubic ($CoPt_{31}$ and $CoPt_{15}$) and tetragonal (Co_2Pt_{10} and CoPt) unit cells were used. The unit cells of the alloys consist of a few vertically and/or horizontally arranged adjacent fcc unit cells, with Co and Pt atoms distributed over nonequivalent atomic positions according to the specific alloy composition. As an example, the unit cells used for cubic $CoPt_7$ and $CoPt_3$ and tetragonal CoPt structures are shown in Fig. 2.

A proper discussion of the electronic transitions underlying the MO spectra requires an analysis of the conductivity tensor of the medium. The off-diagonal components of the optical conductivity tensor $\omega\sigma_{xy}^{(2)}$ were evaluated from the measured complex polar Kerr spectra (polar Kerr rotation and ellipticity) and the complex index of refraction (n and k) in the usual fashion.[5] In Fig. 3(a) the absorptive part of the off-diagonal component of optical conductivity $\omega\sigma_{xy}^{(2)}$ evaluated from experimental data and in Fig. 3(b) the spectra calculated for a selected group of Co-Pt alloys with composition closest to the experimental one are presented. Because the frequency dependence of the optical constants of the alloys is essentially featureless, a close correlation between the Kerr rotation and $\omega\sigma_{xy}^{(2)}$ spectra is observed. The experimental $\omega\sigma_{xy}^{(2)}$ spectra have been scaled by the factors [indicated in Fig. 3(a)] equal to the ratio of their magnetizations at low temperature and at 290 K to take into account the decrease of the Curie temperature of Co_xPt_{1-x} alloys with the decrease of Co content.[37,38] At a first glance, both the theoretical and the experimental spectra exhibit very impressive similarity in the evolution of their spectral features with the change of Co content. However, the experimental peaks are more broad which is due to the existence of a variety of local environments in the disordered phase.[39] Weak but systematic changes in the energy position of the spectral peculiarities can be seen in Fig. 3. There is a slight increase in the energy position of the uv peak with an increase of Co content in the experimental $\omega\sigma_{xy}^{(2)}$ spectra, and even a more pronounced increase in the corresponding theoretical ones. In the ir part of the experimental spectra, the shoulder near 1 eV observed already for $Co_{0.07}Pt_{0.93}$ becomes more prominent with an increase of Co content and transforms into a distinct peak at 1.5 eV in the $Co_{0.48}Pt_{0.52}$ alloy. The same tendency in the evolution of the ir spectral features is observed for the calculated spectra. The $\omega\sigma_{xy}^{(2)}$ spectrum magnitude increases systematically with an increase of Co concentration and exhibits saturation for the CoPt alloy. It is worth noting that the relative amplitudes of the low- and high-energy peaks of the experimental spectra agree well with the theoretical ones in the whole range of investigated Co concentrations. However, the calculated $\omega\sigma_{xy}^{(2)}$ spectra of the Co_xPt_{1-x} alloys are of larger values. The discrepancies can arise due to (i) chemical disorder and the presence of defects in the disordered samples studied (it is known that the MOKE is enhanced in an ordered phase due to modification of Pt-Co coordination in the ordered versus disordered phase[2,10,35]) and (ii) high sensitivity of the optical properties on the sample surface quality (the σ_{xx} spectra evaluated from the measured n and k functions are about 50% smaller as compared to the corresponding calculated spectra which leads to an underestima-

TABLE I. Characterization of the model crystal structures of the Co-Pt alloys assumed in the LMTO calculations. For all structures, alloy composition, type of the structure, space group designation, and group number (Ref. 33), unit cell edges and calculated spin and orbital magnetic moments of Co and Pt (in μ_B) are listed.

Alloy	Structure type	Space group	Lattice constants		M_S		M_L	
			a	c/a	Co	Pt	Co	Pt
Pt	$A1$ [a]	Fm-3m (No. 225)	7.776	1	–	0.160 [b]	–	0.028 [b]
$CoPt_{31}$	–	Pm-3m (No. 221)	7.827	1	1.967	0.051	-0.044	0.001
$CoPt_{15}$	–	Im-3m (No. 229)	7.810	1	1.950	0.085	0.014	0.015
$CoPt_7$	–	Fm-3m (No. 225)	7.776	1	1.941	0.156	0.031	0.033
$CoPt_7$	–	$P4/mmm$ (No. 123)	3.888	2	1.917	0.168	0.022	0.030
$CoPt_7$	–	$P4/mmm$ (No. 123)	7.776	0.5	1.939	0.173	0.036	0.032
Co_2Pt_{10}	–	$P4/mmm$ (No. 123)	3.876	3	1.862	0.201	0.045	0.040
$CoPt_3$	$L1_2$ [a]	Fm-3m (No. 225)	7.706	1	1.736 [c]	0.238 [d]	0.047	0.050
$CoPt_3$	$D0_{22}$	$I4/mmm$ (No. 139)	3.853	2	1.758	0.216	0.019	0.040
$CoPt_3$	$D0_{23}$	$I4/mmm$ (No. 139)	3.853	4	1.777	0.232	0.042	0.048
CoPt	–	P-42c (No. 112)	3.725	2	1.604	0.296	0.052	0.056

[a]The unit cell contains eight standard unit cells.

[b]Calculated at a magnetic field of 920 T.

[c]The calculated and experimental values reported in Refs. 10 and 34 are $1.72\mu_B$ and $(1.64\pm0.04)\mu_B$, respectively.

[d]The calculated and experimental values reported in Refs. 10 and 34 are $0.25\mu_B$ and $(0.26\pm0.02)\mu_B$, respectively.

tion of the magnitude of the $\omega\sigma_{xy}^{(2)}$ spectra evaluated from experimental data).

It is important to point out that for an alloy of a given composition the fine details of the $\omega\sigma_{xy}^{(2)}$ spectrum are sensitive to its actual crystal structure. It is illustrated in Fig. 3(b) for alloys of the same nominal composition $Co_{0.25}Pt_{0.75}$ having different symmetries and local environments of Co and Pt sites. The spectra were calculated for cubic $L1_2$ and tetragonal $D0_{22}$ and $D0_{23}$ crystal structures. As can be seen, the change of an atomic arrangement and accompanying changes of the local symmetry of atomic sites result in the shift of the uv-peak energy position as well as in changes of the relative magnitude of ir and uv maxima of the $\omega\sigma_{xy}^{(2)}$ spectra. Modeling of the chemical disorder by averaging over different configurations[39] would lead to a uv-peak broadening and to less pronounced $\omega\sigma_{xy}^{(2)}$ spectral features and, consequently, to a better agreement with the experimental spectra. The same considerations are also true for alloys of other compositions [not shown in Fig. 3(b)]. It should be noted that in order to account for the effect of a random orientation of microcrystals in the tetragonal structures, the calculated MO spectra were averaged over different orientations of the magnetization with respect to the crystallographic axes according to the approach of Ref. 39.

We should mention that the paramagnetic $Co_{0.035}Pt_{0.965}$ and $Co_{0.049}Pt_{0.951}$ alloys exhibit a maximum at $\sim$1.5 eV in θ_k spectra (corresponding to a minimum in $\omega\sigma_{xy}^{(2)}$), which is not observed in the theoretical spectra. The same frequency dependence in the ir range is observed for Pt metal. The explanation of this behavior is given in Ref. 21 as coming from the intraband contribution to the *off-diagonal* part of the optical conductivity which has not been included in the calculated spectra of Co-Pt alloys. As was shown in Ref. 21 the intraband contribution to σ_{xy} is very small and can usually be neglected in the case of magnetically ordered materials. However, for metals that have zero spontaneous exchange splitting the spin polarization induced by an external magnetic field available in the experiment is small and the contributions of intraband and interband transitions to the off-diagonal component of the optical conductivity tensor can become comparable.

IV. CORRELATION BETWEEN THE ELECTRONIC STRUCTURE AND THE MAGNETO-OPTICAL PROPERTIES

To associate the electronic structure with the MO properties we consider first the changes of the electronic structure with increasing Co content. The well-known characteristic feature of the electronic structure of Co-Pt alloys is the strong hybridization of Co 3d and Pt 5d states, the latter being much more delocalized. Figure 4 shows the calculated spin- and site-projected densities of the electronic states (DOS) for Co and Pt sites in $CoPt_7$, $CoPt_3$, and CoPt alloys. The DOS for fcc Pt calculated in the magnetic field of 920 T is considered here and henceforth as a reference system (this value of magnetic field is needed to induce the Pt magnetic moment of $0.16\mu_B$ close to the average Pt moment calculated for ferromagnetic $CoPt_7$ alloy). As is seen, the electronic structure depends strongly on the alloy composition. This is the result of the strong dependence of hybridization details between Co 3d and Pt 5d states on the number of

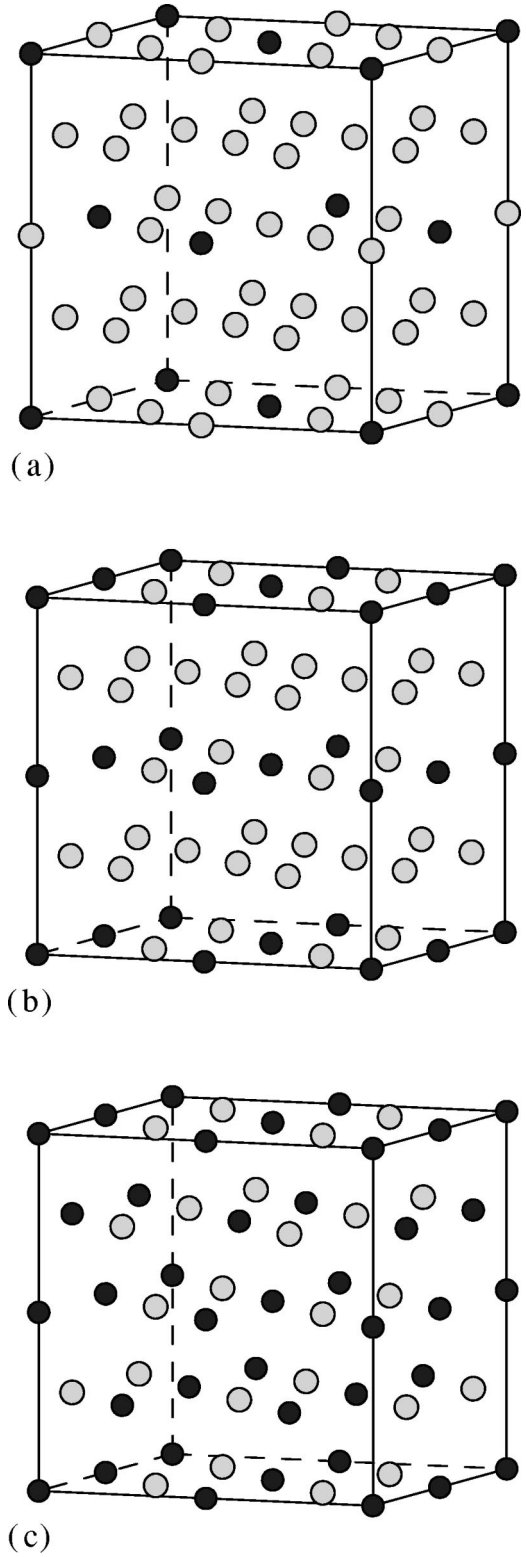

FIG. 2. Unit cells used for (a) Co_1Pt_7 (Fm-3m), (b) Co_1Pt_3 (Fm-3m), and (c) Co_1Pt_1 (P-42c) alloys.

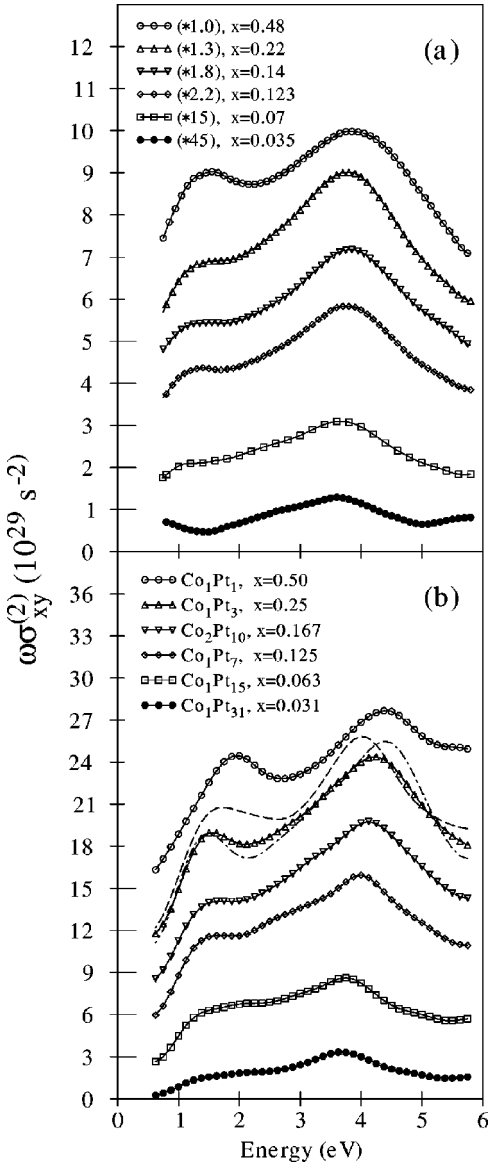

FIG. 3. The comparison of the absorptive part of the off-diagonal component $\omega\sigma_{xy}^{(2)}$ of the optical conductivity tensor, determined from the ellipsometric and the complex polar Kerr angle measurements for Co_xPt_{1-x} alloys ($x=0.035$, 0.07, 0.123, 0.14, 0.22, and 0.48) (a) with the spectra calculated for the model $CoPt_{31}$, $CoPt_{15}$, $CoPt_7$, Co_2Pt_{10}, $CoPt_3$, and CoPt alloys (b) (the corresponding alloy compositions are given in the legend). In the panel (b) triangles and dashed and dash-dotted lines denote the spectra of $D0_{22}$, $D0_{23}$, and $L1_2$ structures, respectively. The spectra marked with solid circles are to scale; all other spectra are shifted by a constant offset of 1 and 3×10^{29} s^{-2} towards each other in panels (a) and (b), respectively.

nearest Pt(Co) neighbors for each Co(Pt) atom. Pt lends its strong spin-orbit coupling to the system while inside Co atomic spheres the effect of the spin-orbit coupling is much weaker than the effect of the exchange field. The electronic states at the bottom of the valence band are formed mainly by Pt states. The high density of both Pt 5d and Co 3d states in the energy range from -3.5 to 1.0 eV suggests a high degree of hybridization between them. However, as compared to the spin-up states the spin-down ones are hybridized to a far lesser extent. On the contrary, in the vicinity of the Fermi energy (E_F) stronger hybridization occurs for the spin-down states. With the increase of Co content in Co_xPt_{1-x} alloys the hybridization of Pt states with the

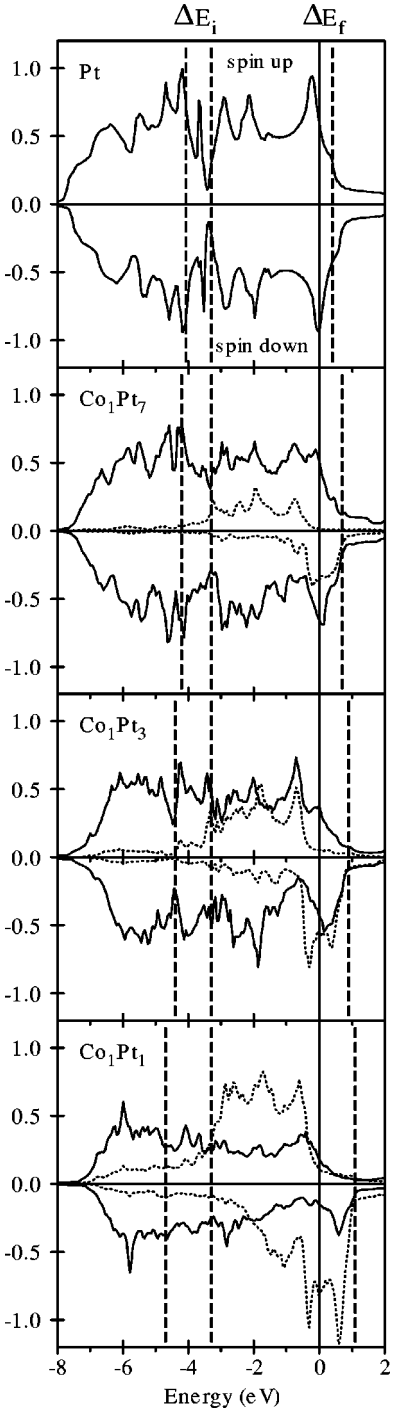

FIG. 4. Spin-projected densities of Pt (solid line) and Co (dotted line) *d* states [in electrons/(unit cell eV)] calculated for fcc Pt in a magnetic field of 920 T, $CoPt_7$, $CoPt_3$, and CoPt alloys. The vertical dashed lines indicate the energy windows for initial and final states ΔE_i and ΔE_f (see text) and the vertical solid line marks the Fermi level.

exchange-split Co states increases. This leads to an increase of the difference in occupation of Pt majority and minority spin states and, as a consequence, of the magnetic moment induced on the Pt site which approaches the value of $0.3\mu_B$ for the alloy of equiatomic composition. On the contrary, the magnetic moment on Co atoms decreases. The compositional dependence of the average value of the Co and Pt spin magnetic moments is presented in Table I. It has been verified that, as opposed to the magnetic moments, the spin-orbit coupling strength on Pt sites is much less sensitive to the alloy composition and changes only within 2.5% for Pt $5d$ states which agrees with the observation reported in Ref. 13. Thus, although the SO interaction plays a crucial role in the formation of the MO response,[40] one can conclude that the dependence of the MO spectra of the Co_xPt_{1-x} alloys on the Co content is hardly related to the changes of the Pt SO coupling strength but rather to the change of the hybridization and to increased Pt exchange splitting.

A. Decomposition of the $\omega\sigma_{xy}(\omega)$ spectra

To examine and identify the energy position of the initial and final states responsible for the main spectral features in Co_xPt_{1-x} alloys and their relation with that of Pt metal, an analysis of the transitions arising between different narrow energy ranges has been performed. We decomposed the calculated $\omega\sigma_{xy}(\omega)$ spectra into contributions coming from the initial states lying in different energy ranges below the Fermi level to all final states, as well as into contributions coming from all initial states to the states lying in different energy intervals above E_F.

In Figs. 5(a)–5(d) the contributions to the $\omega\sigma_{xy}(\omega)$ spectra of the $CoPt_7$, $CoPt_3$, and CoPt alloys and to the spectrum of strongly magnetized Pt coming from the initial states located within well-defined energy windows are shown. The dashed lines in Figs. 5(a)–5(d) denote the contribution coming from a 0.8-eV-wide energy interval of the initial states just below E_F to all possible final states. For all compounds these transitions give an almost constant off-diagonal optical conductivity in the 2–6 eV photon energy range. The solid lines in Figs. 5(a)–5(d) show the contribution coming from the occupied states situated within an energy interval ΔE_i between -4.2 and -3.4 eV in Pt which extends down to -4.8 eV in CoPt. In Figs. 5(e)–5(h) the results of the analysis of transitions coming from all possible initial states to different final states are presented. It was found that a relatively narrow energy window ΔE_f lying just above E_F and equal to 0.3, 0.6, 0.8, and 1.0 eV for Pt, $CoPt_7$, $CoPt_3$, CoPt, respectively, can be specified. The transitions to the final states within ΔE_f are responsible for the main spectral features of $\omega\sigma_{xy}(\omega)$, i.e., the peaks in the ir and uv regions. The transitions to the final states lying above ΔE_f give both for Pt and for Co_xPt_{1-x} alloys merely a more or less constant contribution in the 2–6 eV photon energy range.

It should be noted that for all alloys studied an additional peak arises at $\hbar\omega = 1$–2 eV in the $\omega\sigma_{xy}(\omega)$ spectra, the amplitude of which increases with increasing Co content. It was found that the ir peak comes from the transitions between initial states located in the energy range from -1.9 to -0.8 eV to the states within the ΔE_f window just above E_F. The energy windows coincide well with those responsible for the ir peak of pure fcc Co. However, it was found that the $\omega\sigma_{xy}(\omega)$ spectrum of Co cannot be described by the same kind of contributions as in the alloys studied.

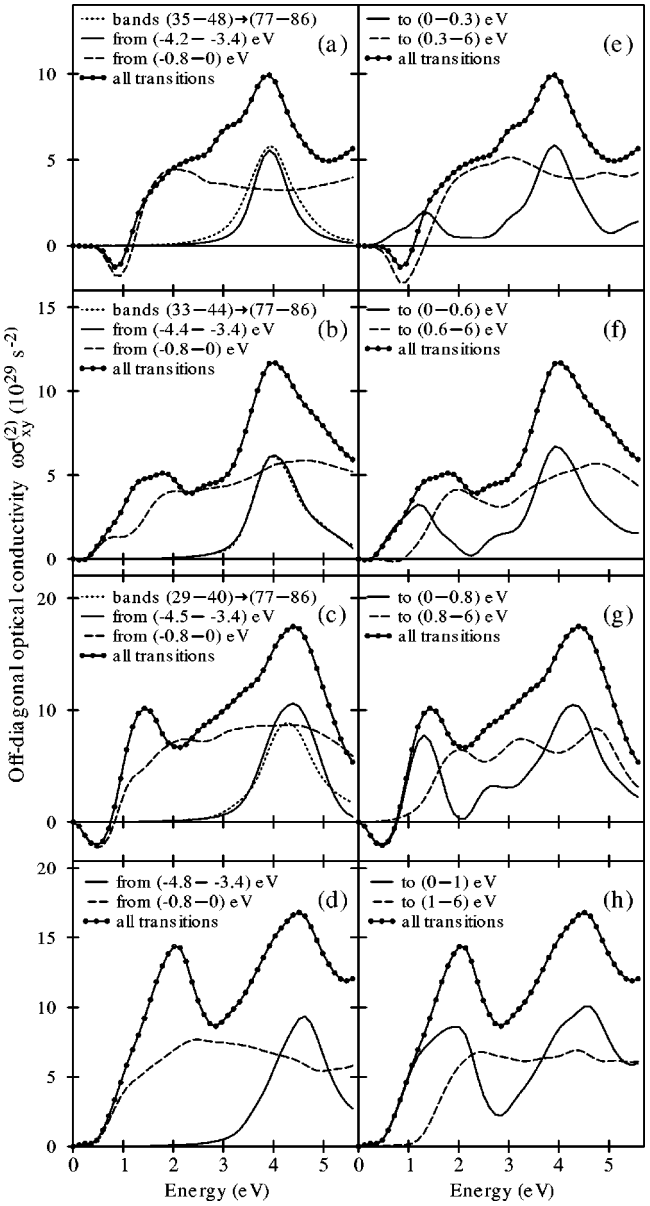

FIG. 5. Calculated $\omega\sigma_{xy}^{(2)}$ spectra (solid lines with circles) of fcc Pt in a magnetic field of 920 T (a), $CoPt_7$ (b), $CoPt_3$ (c) and CoPt (d) alloys. Solid and dashed lines show the contributions from the initial states localized within the indicated intervals (in eV) below the Fermi energy to all final states (left panels) and from all initial to those final states that are localized within the indicated intervals (right panels). Dotted lines denote the transitions between the groups of initial and final bands. Their numbers are given in parentheses in the legend.

From the analysis of the decomposed spectra the conclusion, valid for all the examined Co_xPt_{1-x} alloys as well as for Pt metal, can be derived that the $\omega\sigma_{xy}(\omega)$ spectra above 2 eV can be represented with a good accuracy as a sum of two contributions.

(a) The pronounced peak at 4 eV in the $\omega\sigma_{xy}(\omega)$ spectra which is almost exclusively determined by the interband transitions from the deep-lying occupied states within the relatively narrow energy interval ΔE_i equal to 0.8, 1.0, 1.1, and 1.4 eV for Pt, $CoPt_7$, $CoPt_3$, and CoPt, respectively, to the unoccupied states spanning the energy interval ΔE_f. These energy intervals responsible for the MO peak at 4 eV are indicated by vertical dashed lines in Fig. 4.

(b) The weakly energy-dependent in the 2–6 eV photon energy range contribution to the $\omega\sigma_{xy}(\omega)$ coming from the transitions between the occupied states lying in the energy window -0.8 to E_F eV and the unoccupied states located above ΔE_f.

Broadly speaking, the overall spectral shape of both contributions discussed above looks similar and remains close to that observed in Pt, but their magnitude changes considerably with Co content. This observation can be explained on the basis of simple considerations that the increase of the Co-Pt alloy spectra magnitude with an increase of Co content is related mainly to the increase of Pt exchange splitting due to direct hybridization between Pt orbitals and spin-polarized Co orbitals. As was shown in Ref. 21, the MO spectra amplitude of Pt metal scales in a wide range with induced magnetic moment. This is definitely seen in Figs. 5(a) and 5(b), where the same magnetic moment on Pt sites in $CoPt_7$ alloy and Pt metal in the external magnetic field results in a comparable amplitude of the contributions to the $\omega\sigma_{xy}(\omega)$ spectra. We found that the conclusion qualitatively holds also in the case of $CoPt_3$ and CoPt alloys. The origin of the behavior can be understood because in spite of the low magnetic moment of $(0.16–0.3)\mu_B$ on Pt as compared to $(1.9-1.6)\mu_B$ on Co, due to the large spin-orbit coupling the amplitude of the $\omega\sigma_{xy}(\omega)$ spectra of Pt in the uv range is 3–4 times larger as compared to that of fcc Co. This conclusion is consistent with the results of test calculations obtained with manipulation of the SO coupling strength on a Pt site in Co-Pt alloys.[2,5] It has been verified that, even in the case of CoPt alloy, the $\omega\sigma_{xy}(\omega)$ spectra amplitude after switching off the SO coupling on Pt decreases to $\sim$10% in the uv range and to $\sim$30% in the ir range.

The above explanation can be considered as giving only a rough, qualitative estimate of the $\omega\sigma_{xy}(\omega)$ spectra. The distinctions between the shapes of the spectra in different spectral regions arise with changes of alloy composition [Figs. 5(a) and 5(d)]. In particular, the peak at 4 eV has almost a symmetric shape in Pt but rather an asymmetric one in the alloys. The distinctions in the fine structure of the spectra come from the fact that the $\omega\sigma_{xy}(\omega)$ spectra of Co_xPt_{1-x} alloys cannot be represented by simple superpositions of Co and Pt contributions, but depend on details of the band structure which are influenced by various factors such as the alloy composition, the lattice symmetry, and the local environment of Co and Pt atoms. These details can be only investigated by analysis of the evolution of the band structure of the alloys with the change of Co content.

B. Correlation between the band structure and the MO peak at 4 eV

It is well known that the optical and MO spectra reflect information on both the initial and final states simultaneously (joint density of states). Besides, they are strongly influenced by the optical transition matrix elements, which in the case

of the MO spectra depend on the spin and orbital polarization of the initial and final states.

To illustrate the influence of the spin-orbit interaction on the initial and final states involved in the transitions let us introduce a site-dependent function $dm_{tl}(E)$ given by[24]

$$dm_{tl}(E)=\sum_{n\mathbf{k}} \langle \Psi_{tl}^{n\mathbf{k}}|\hat{l}_z|\Psi_{tl}^{n\mathbf{k}}\rangle \delta(E-E_{n\mathbf{k}}), \qquad (1)$$

where $\hat{l}_z$ is the z projection of the angular momentum operator, and $E_{n\mathbf{k}}$ and $\Psi_{tl}^{n\mathbf{k}}$ are the energy of the nth band and the part of the corresponding LMTO wave function formed by the states with angular momentum l inside the atomic sphere centered at site t, respectively. In analogy to the l-projected density of states, $dm_{tl}(E)$ can be referred to as site- and l-projected density of the expectation value of $\hat{l}_z$. This quantity has purely relativistic origins and when the SO interaction is equal to zero, $dm_{tl}(E)\equiv 0$. As van Vleck[41] showed for a free ion, the absence of orbital degeneracy is a sufficient condition for the quenching of the orbital moment, which means that the first-order contribution should vanish: $\langle \Psi_{\mathbf{k}}|\hat{l}_z|\Psi_{\mathbf{k}}\rangle=0$. Thus, $dm_{tl}(E)$ can be considered as the measure of the SO interaction of the electronic states. One can expect that the electronic states for which the magnitude of the $dm_{tl}(E)$ function is large should give a strong contribution to the MO spectra. Due to the dipole selection rules, only the electronic states with an appropriate symmetry contribute to the spectra. In our case the most important are the interband transitions between d and p states. Figures 6(a)–6(f) present the Co and Pt site-projected $dm_l(E)$ functions for $l=1$ and $l=2$ orbital quantum numbers calculated for $CoPt_7$ and $CoPt_3$ (fcc Pt is also included for comparison). Let us concentrate our attention on the electronic states which give the largest contribution to the prominent 4 eV peak in the off-diagonal optical conductivity indicated by vertical dashed lines in Figs. 6 and 4. As has been shown the peak at 4 eV is determined by transitions to the final states in the window ΔE_f just above the Fermi level which are predominantly of Pt and Co d character. With an increase of Co content the magnitude of both Co and Pt $dm_{l=2}(E)$ increases appreciably in this range. The initial states for these transitions lie in the narrow energy interval ΔE_i below -3.4 eV and, due to the dipole selection rules, are mainly of p character. Remarkably, the $dm_l(E)$ for Pt p states reaches its maximal magnitude exactly in the same energy range. Going from fcc Pt to the $CoPt_3$ alloy one can note that the structure of the peak becomes more complex but its position remains approximately the same. The change of the $dm_l(E)$ shape in this energy range reflects to some extent the change of the Pt-d–Co-d hybridization. An indication for this is the appearance of the peak in the $dm_l(E)$ of Co d states at the border of the energy window ΔE_i. The qualitative analysis discussed above can serve as a tool for the determination of the initial and final states most probable for the MO-active interband transitions.

To find a direct correlation between the $\omega\sigma_{xy}^{(2)}$ spectra of Co-Pt alloys and corresponding band structure, in the following discussion we focus our attention particularly on the origin of the pronounced peak at 4 eV by identifying the initial and final states involved and their **k**-space localization. It is obvious that the interpretation of the MO spectra of complex compounds in terms of electronic transitions is quite a complicated problem. The initial and final states involved in optical transitions of Co-Pt systems are hybridized states and their wave functions are delocalized. Moreover, in the formation of the optical as well as magneto-optical spectra of the medium, the matrix elements of the interband transitions and selection rules are also of great importance. In principle, to compare directly band structures of different alloys with that of fcc Pt metal, we should use crystal structures with the same symmetry group and the same number of atoms per unit cell and, therefore, the same type of Brillouin zone. So, for this aim, we chose as a basic lattice the face-centered-cubic lattice of $CoPt_7$ alloy of Fm-3m space group. The primitive rhombohedral cell in this case contains 8 atoms and the cubic unit cell containing 32 atoms is shown in Fig. 2(a). In such a representation, the corresponding cubic unit cell of fcc Pt has a doubled dimensions and contain 8 standard fcc $A1$ unit cells, and that of the $CoPt_3$ alloy [Fig. 2(b)] 8 standard $L1_2$ unit cells of Cu_3Au-type structure. Unfortunately,

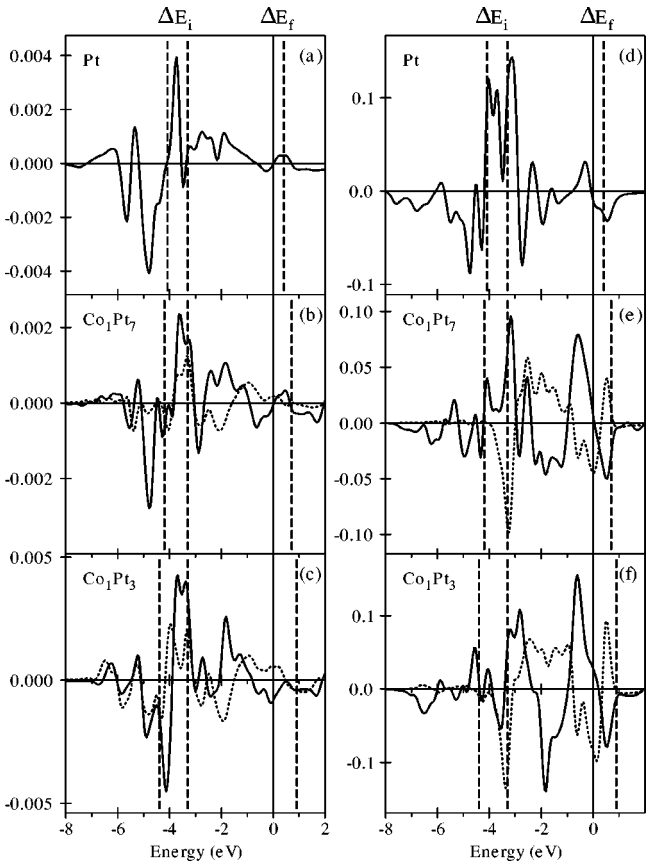

FIG. 6. Density of the expectation value of $\hat{l}_z$ for Pt (solid line) and Co (dotted line) states with $l=1$ (left panels) and $l=2$ (right panels) orbital quantum numbers in fcc Pt in a magnetic field of 920 T, $CoPt_7$, and $CoPt_3$ alloys [in electrons/(unit cell eV)]. The vertical dashed lines indicate the energy windows for initial and final states ΔE_i and ΔE_f (see text) and the vertical solid line marks the Fermi level.

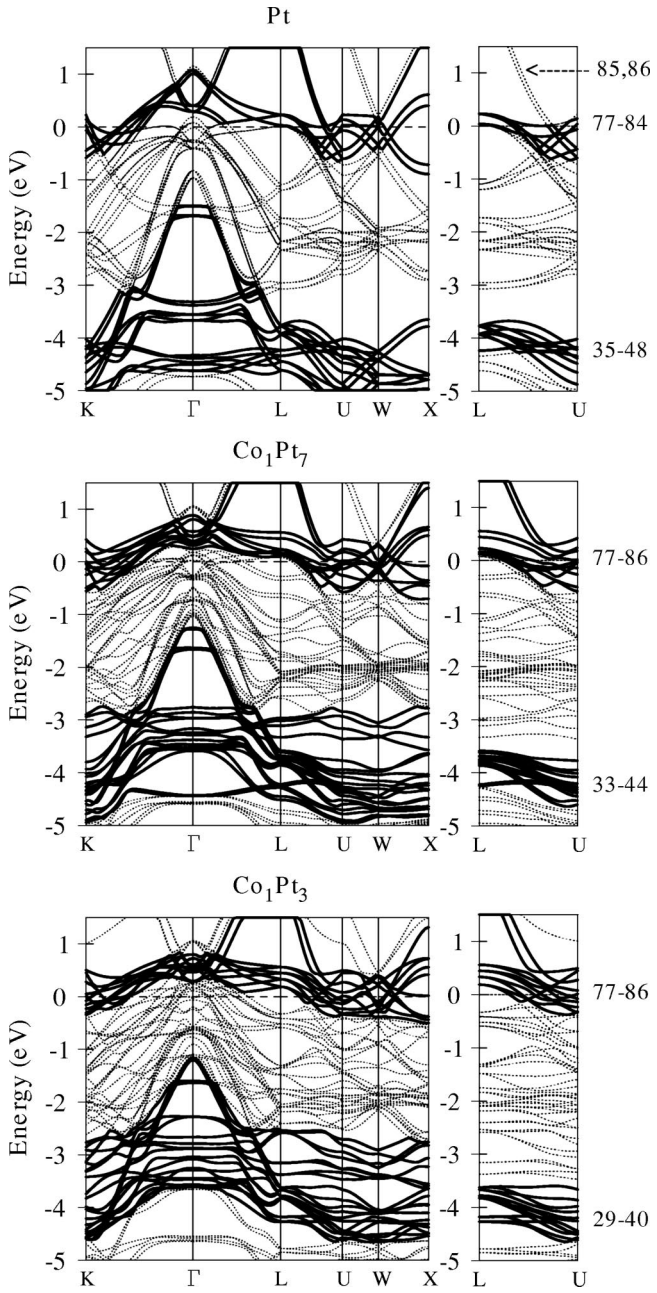

FIG. 7. Fully relativistic spin-polarized band structure of fcc Pt in a magnetic field of 920 T and $CoPt_7$ and $CoPt_3$ alloys. Solid thick lines at the left panels indicate the groups comprising the most MO-active initial and final bands. Solid thick lines at the right panels indicate the most MO active bands in the *L*-*U* symmetry direction of the Brillouin zone, with the band numbers indicated at the right-hand side.

we were not able to construct a corresponding face-centered-cubic unit cell of the enlarged volume for CoPt alloy.

Figure 7 shows the calculated band structures of Pt, $CoPt_7$, and $CoPt_3$ alloys along symmetry lines of the Brillouin zone. To illustrate the evolution of the band structure with the increase of Co content, in Fig. 7 we selected (the same for each case) two group of bands (initial, from 29 to 48, and final, – from 77 to 86) by denoting them by thick solid lines (we will see further that optical transitions among those groups of bands are responsible for the MO peak in uv at ~ 4 eV). From Fig. 7, the conclusion can be drawn that upon increasing the Co content the band splitting increases, and a strong shift of the occupied energy band positions to higher energy as a results of the Co($3d$)-Pt($5d$) hybridization effects takes place. Looking at the band structure, it is definitely seen in Fig. 7 that, as one proceeds from pure paramagnetic Pt to $CoPt_7$ and $CoPt_3$ alloys, the hybridization of the electronic states increases. This is clearly seen, for example, in the right panels of Fig. 7 from the $E(\mathbf{k})$ dependence of the 85,86 bands. In Pt, these energy bands almost do not hybridize, with low-lying bands having rather large $\nabla_{\mathbf{k}} E(\mathbf{k})$ around the *U* symmetry point. They simply cross the 83,84 bands without any repulsion. In $CoPt_7$ and $CoPt_3$ alloys, the Co electronic states hybridize with the Pt states. As a result of the band repulsion, these states spread over the energy scale up to ~ 0.5 eV, whereas $\nabla_{\mathbf{k}} E(\mathbf{k})$ becomes almost equal to zero at the *U* point in $CoPt_3$ alloy. Similar effects of energy level repulsion with accompanying mixing—hybridization—of states after quantum-mechanical crossing of levels can be seen in Fig. 7 in the whole Brillouin zone. Due to Pt($5d$)-Co($3d$) hybridization, the $E(\mathbf{k})$ slopes of the initial and final states become more similar around selected symmetry points, which leads to both an increase of the joint density of states and oscillator strengths of the optical transitions. Another important effect that strongly affects the MO spectra in Co_xPt_{1-x} alloys with increasing concentration of Co is a reduction of the Fermi energy due to the fact that Co has fewer valence electrons in comparison with Pt. The deoccupation of the energy bands by electrons due to a decrease of the Fermi level involves additional final states into interband transitions which also increases the intensity of the transitions.

To identify which kind of interband transitions and parts of the Brillouin zone are responsible for the prominent peak at 4 eV, we performed a **k**-space decomposition of the interband transitions into transitions occurring in the vicinity of the high-symmetry points of the Brillouin zone. This was accomplished via a theoretical analysis of about 8000–10 000 individual interband transitions in high-symmetry points and lines of the BZ. For this aim, we summed all transitions between the bands *n* and *m* in a cubic volume surrounding a given point with a cube edge equal to 1/6 of the Γ-*X* distance (it contains approximately 4.5% of a whole BZ volume). Although the results depend on the volume of the cube, one can identify the transitions essentially with these points and their nearest neighborhood. A detailed analysis of the contributions shows that in both Pt and Co-Pt alloys the $\sigma_{xy}^{(2)}$ spectra are determined by transitions at the BZ edge along the Γ-*L*, *L*-*U*, and *U*-*W* symmetry directions. It was found that the most intensive transitions responsible for the MO peak at 4 eV come from the states located on the *L*-*U* symmetry direction. The initial and final bands for these transitions are marked by solid thick lines in the right panels of Fig. 7. Moreover, in the alloys the peak observed in the ir range is formed by the transitions between the hybridized states in the Γ-*L*-*U* symmetry plane.

It was identified that the transitions from the bands (35–48), (33–44), and (29–40) in Pt, $CoPt_7$, and $CoPt_3$, respec-

tively, to the same specified group of empty bands (77–86) are responsible for the pronounced peak at 4 eV in MO spectra. The intensity of these transitions [marked by dotted lines in Figs. 5(a)—5(c)] almost coincides with the intensity of the peak derived from the ΔE_i and ΔE_f energy windows. It should be pointed out that when the Co content increases, the alloy *d*-band width systematically decreases (see Figs. 4 and 7) and the deep-lying initial bands shift to higher energy, giving, as was found, a significant contribution to the peak at 4 eV.

It was verified that the intensities of interband transitions from the analyzed initial states to individual final bands increase with Co content. In particular, the transitions to the (85,86) final bands contribute only about 2% to the total intensity of the pronounced peak in pure Pt, but their contributions increase to about 10% and 25% in $CoPt_7$ and $CoPt_3$ alloys, respectively. The high increase of the intensity of the transitions to unoccupied (85,86) bands is a good illustration of the role of the hybridization. The Pt($5d$)-Co($3d$) hybridization effects that determine the details of the band structure of the alloys are responsible also for the increase of the intensity of the second contribution (i.e., transitions from the window just below E_F to all final states) with an increase of the Co content. To study the influence of the spin-orbit and the exchange splitting on the band structure of Co-Pt alloys, we performed test calculations through manipulation of the magnitude of the interaction on a particular site. We found that the deep-lying initial states undergo the largest changes with a change of the spin-orbit coupling strength, whereas the empty bands are more sensitive to the influence of the exchange splitting arising as a result of hybridization between Pt and Co wave functions.

Although details of the band structure change dramatically upon an increase of Co content, it should be noted that the structure of the peak at 4 eV changes only weakly and remains close to that of Pt metal. To understand the close resemblance between the peak at 4 eV in paramagnetic Pt and in Co-Pt alloys, we examined the role of the final states involved in the transitions. In both cases the final states responsible for the peak at 4 eV are located within a very close energy range in the vicinity of E_F and within the same part of **k** space. It was found that an increase of band splitting by the external magnetic field in Pt or due to the direct hybridization (between Pt orbitals and spin-polarized Co orbitals) mechanism in alloys results mainly in changes of the occupation of the bands at the Fermi level (i.e., the density of empty spin-down states increases). Thus, the evolution of the $\omega\sigma_{xy}^{(2)}$ spectra of Co-Pt alloys with composition in the range studied can be qualitatively considered as due to a similar mechanism as in the case of the induced spin polarization in pure Pt in an external magnetic field, notwithstanding that the characters of the final as well as the underlying initial states are different.

In conclusion, the individual interband $n \rightarrow m$ transitions arising from the vicinity of the same **k** points characterize essentially the same MO spectral shape in Pt and Co-Pt alloys. On the other hand, the differences in the band structure of Pt and Co-Pt alloys due to the different position of the Fermi level and different degree of Co-$3d$–Pt-$5d$ hybridization result in different intensities of the individual transitions that sum up to basically similar but different in details MO spectra of Pt and Co-Pt alloys.

V. SUMMARY

We have studied, both experimentally and theoretically, the magneto-optical spectral properties for a series of disordered Co_xPt_{1-x} alloys. The electronic structure and the MO properties of the alloys in comparison with that of fcc Pt metal in an external magnetic field were investigated by means of the *ab initio* fully relativistic spin-polarized LMTO method. It was shown that the spectral dependence and the main spectral features of the measured MO spectra are reproduced in a very satisfying way by calculations within the supercell approach for a wide range of alloy concentrations from $x=0.03$ up to $x=0.5$.

In this work, a complete study of the correlation between the electronic structure and the MO properties of the systems is presented. The importance of the spin-orbit interaction for transitions in different energy regions is demonstrated by calculating the density of the expectation value of the orbital moment. The microscopic origin of the characteristic for the Co-Pt alloys prominent peak in the uv range in the MO spectra at 4 eV photon energy was investigated in detail. It was found that the Kerr rotation and the $\sigma_{xy}^{(2)}$ spectra of Pt and Co-Pt alloys are mainly determined by two contributions. The prominent peak at 4 eV photon energy mostly comes from the interband transitions from occupied states within a relatively narrow energy interval ΔE_i lying at -3.4 eV below the Fermi level ($\Delta E_i=0.8$, 1.0, 1.1, and 1.4 eV) to another narrow interval ΔE_f just above the Fermi level ($\Delta E_f=0.3$, 0.6, 0.8, and 1.0 eV for Pt, $CoPt_7$, $CoPt_3$, and CoPt alloys, respectively). The band-by-band and **k**-space decomposition of the MO spectra were performed and the transitions responsible for the 4 eV peak in the spectra were identified. It was found that in Pt as well as in the Co-Pt alloys these interband transitions are localized essentially around the same **k** points. Moreover, the interband transitions at the edge of the Brillouin zone, namely, along the Γ-L, L-U, and U-W symmetry directions, play a crucial role in the formation of the MO spectra of Co-Pt alloys of different composition.

Although the fine details of the MO spectra of the Co_xPt_{1-x} alloys for x up to 0.5 depend on the details of the spin-polarized band structure, the characteristic enhancement of the spectra in the uv range can be considered as coming mainly from spin-polarized Pt. The comparative analysis of the off-diagonal optical conductivities in Pt and Co-Pt alloys clearly demonstrates that MO spectroscopy is a very sensitive method to investigate minor differences in the electronic structure of solids.

ACKNOWLEDGMENT

V.N.A. gratefully acknowledges the hospitality during his stay at the Institute of Experimental Physics, University of Bialystok.

*To whom any correspondence should be addressed. Electronic address: ubaluba@venus.uwb.edu.pl

†Permanent address: Institute of Metal Physics, 36 Vernadskii Street, 252142 Kiev, Ukraine.

[1] T. Massalski, *Binary Alloy Phase Diagrams* (American Society for Metals, Metals Park, OH, 1990), Vol. 2.

[2] G. R. Harp, D. Weller, T. A. Rabedeau, R. F. C. Farrow, and R. F. Marks, in *Magnetic Ultrathin Films-Multilayers and Surfaces, Interfaces and Characterization*, edited by B. T. Jonker, S. A. Chambers, R. F. C. Farrow, C. Chappert, R. Clarke, W. J. M de Jonge, T. Egami, P. Grünberg, K. M. Krishnan, E. E. Marinero, C. Rau, and S. Tsunashima, Mater. Res. Soc. Symp. Proc. No. **313** (Materials Research Society, Pittsburgh, 1993), p. 493; D. Weller, J. Sticht, G. R. Harp, R. F. C. Farrow, R. F. Marks, and H. Brändle, *ibid.*, p. 501.

[3] G. R. Harp, D. Weller, T. A. Rabedeau, R. F. C. Farrow, and M. F. Toney, Phys. Rev. Lett. **71**, 2493 (1993).

[4] S. Uba, L. Uba, R. Gontarz, V. N. Antonov, A. Ya. Perlov, and A. N. Yaresko, J. Magn. Magn. Mater. **140-144**, 575 (1995).

[5] S. Uba, L. Uba, A. N. Yaresko, A. Ya. Perlov, V. N. Antonov, and R. Gontarz, Phys. Rev. B **53**, 6526 (1996).

[6] G. Y. Guo and H. Ebert, J. Magn. Magn. Mater. **156**, 173 (1996).

[7] P. M. Oppeneer, V. N. Antonov, T. Kraft, H. Eschrig, A. N. Yaresko, and A. Ya. Perlov, J. Phys.: Condens. Matter **8**, 5769 (1996).

[8] E. T. Kulatov, Yu. A. Uspenskii, and S. V. Halilov, J. Magn. Magn. Mater. **163**, 331 (1996).

[9] S. Iwata, S. Yamashita, and S. Tsunashima, IEEE Trans. Magn. **MAG-33**, 3670 (1997).

[10] R. J. Lange, S. J. Lee, D. W. Lynch, P. C. Canfield, B. N. Harmon, and S. Zollner, Phys. Rev. B **58**, 351 (1998).

[11] M. Yamaguchi, T. Kusakabe, K. Kyuno, and S. Asano, Physica B **270**, 17 (1999).

[12] H. Miyazawa and T. Oguchi, J. Phys. Soc. Jpn. **68**, 1412 (1999).

[13] M. Kim, A. J. Freeman, and R. Wu, Phys. Rev. B **59**, 9432 (1999).

[14] G. S. Chang, C. N. Whang, J. Y. Rhee, and Y. P. Lee, J. Appl. Phys. **87**, 1775 (2000).

[15] A. Cebollada, D. Weller, J. Sticht, G. R. Harp, R. F. C. Farrow, R. F. Marks, R. Savoy, and J. C. Scott, Phys. Rev. B **50**, 3419 (1994).

[16] G. Armelles, D. Weller, B. Rellinghaus, R. F. C. Farrow, M. F. Toney, P. Caro, A. Cebollada, and M. I. Alonso, IEEE Trans. Magn. **MAG-33**, 3220 (1997).

[17] D. Weller, W. Reim, K. Spörl, and H. Brändle, J. Magn. Magn. Mater. **93**, 183 (1991).

[18] K. Sato, H. Ikekame, Y. Tosaka, K. Tsuzukiyama, Y. Togami, and M. Fujisawa, J. Magn. Magn. Mater. **126**, 572 (1993).

[19] P. Kielar, M. Nyvlt, V. Parizek, V. Prosser, Š. Višňovský, R. Krishnan, and M. Tessier, J. Appl. Phys. **73**, 6115 (1993).

[20] L. Uba, S. Uba, A. N. Yaresko, A. Ya. Perlov, V. N. Antonov, and R. Gontarz, J. Magn. Magn. Mater. **193**, 159 (1999).

[21] L. Uba, S. Uba, V. N. Antonov, A. N. Yaresko, and R. Gontarz, Phys. Rev. B **62**, 16 510 (2000).

[22] L. Smardz, J. Baszynski, and B. Rauschenbach, Thin Solid Films **175**, 295 (1989).

[23] K. Sato, Jpn. J. Appl. Phys., Part 1 **20**, 2403 (1981).

[24] L. Uba, S. Uba, V. N. Antonov, A. N. Yaresko, T. Ślęzak, and J. Korecki, Phys. Rev. B **62**, 13 731 (2000).

[25] D. E. Aspnes and A. A. Studna, Appl. Opt. **14**, 220 (1975).

[26] O. K. Andersen, Phys. Rev. B **12**, 3060 (1975).

[27] V. V. Nemoshkalenko and V. N. Antonov, *Computational Methods in Solid State Physics* (Gordon and Breach, London, 1998).

[28] H. Ebert, Phys. Rev. B **38**, 9390 (1988).

[29] V. N. Antonov, A. I. Bagljuk, A. Ya. Perlov, V. V. Nemoshkalenko, Vl. N. Antonov, O. K. Andersen, and O. Jepsen, Fiz. Nizk. Temp. **19**, 689 (1993) [Low Temp. Phys. **19**, 494 (1993)].

[30] G. Y. Guo and H. Ebert, Phys. Rev. B **51**, 12 633 (1995).

[31] P. E. Blöchl, O. Jepsen, and O. K. Andersen, Phys. Rev. B **49**, 16223 (1994).

[32] H. Brändle, D. Weller, J. C. Scott, S. S. P. Parkin, and C.-J. Lin, IEEE Trans. Magn. **MAG-28**, 2967 (1992).

[33] *International Tables for Crystallography*, edited by T. Hahn (Reidel, Dordrecht, 1983), Vol. A.

[34] F. Menzinger and A. Paoletti, Phys. Rev. **143**, 365 (1966).

[35] A. L. Shapiro, P. W. Rooney, M. Q. Tran, F. Hellman, K. M. Ring, K. L. Kavanagh, B. Rellinghaus, and D. Weller, Phys. Rev. B **60**, 12 826 (1999).

[36] R. Gontarz, T. Lucinski, L. Uba, S. Uba, and Yu. V. Kudryavtsev, Acta Phys. Pol. A **85**, 427 (1994).

[37] *Magnetic Properties of Metals: 3d, 4d and 5d Elements, Alloys and Compounds*, edited by H. P. J. Wijn, Landolt-Börnstein, New Series, Group III, Vol. 19a (Springer, Berlin, 1992), p. 616.

[38] D. Weller, H. Brändle, and C. Chappert, J. Magn. Magn. Mater. **121**, 461 (1993).

[39] S. Uba, A. N. Yaresko, L. Uba, A. Ya. Perlov, V. N. Antonov, R. Gontarz, and H. Ebert, Phys. Rev. B **57**, 1534 (1998).

[40] H. S. Bennett and E. A. Stern, Phys. Rev. **137**, A448 (1965).

[41] J. H. van Vleck, *Electric and Magnetic Susceptibilities* (Oxford University Press, Oxford, 1932).